JOURNAL OF AIRCRAFT
Vol. 32, No. 3, May–June 1995

Engineering Notes

ENGINEERING NOTES are short manuscripts describing new developments or important results of a preliminary nature. These Notes cannot exceed 6 manuscript pages and 3 figures; a page of text may be substituted for a figure and vice versa. After informal review by the editors, they may be published within a few months of the date of receipt. Style requirements are the same as for regular contributions (see inside back cover).

Optimal Trajectories for an Unmanned Air-Vehicle in the Horizontal Plane

Joseph Z. Ben-Asher*
Taas-Israel Industries, Ltd.,
Ramat-Hasharon 47100, Israel

Nomenclature

$A1, A2, A3$	=	propulsion coefficients
$Cd0$	=	drag coefficient
D	=	drag
Di	=	induced drag
$D0$	=	zero-lift drag
e	=	specific energy
H	=	Hamiltonian
h	=	altitude
K	=	induced-drag factor
k	=	propulsion factor
n	=	load factor
Pt	=	total pressure
$P0$	=	sea-level pressure
q	=	dynamic pressure
S	=	reference area
Tf	=	final time
Th	=	thrust
Tt	=	total temperature
$T0$	=	sea-level temperature
t	=	time
V	=	velocity
W	=	weight
x	=	range
$\bar{x}$	=	state vector $(x, y, e, \Psi)^T$
y	=	cross-range
$\bar{\lambda}$	=	costate vector, $(\lambda_x, \lambda_y, \lambda_e, \lambda_\Psi)^T$
Φ	=	bank angle
Φ_{max}	=	maximum bank angle
Φ_{min}	=	minimum bank angle
Ψ	=	azimuth angle

Introduction

TIME-OPTIMAL trajectories in the horizontal plane for a thrusting vehicle have been investigated quite extensively in the past 35 yr.[1–3] The present work employs some modern computational techniques in order to investigate these trajectories for an actual unmanned air-vehicle (UAV) called DELILAH. DELILAH is a small turbojet-powered decoy equipped with active and passive rf payloads to simulate a full-size aircraft. It weighs 400 lb, its dash speed is about 770 fps, its stall speed is about 250 keas, and its flight ceiling is 30,000 ft. Minimum-time flight trajectories in the vertical plane for the same air-vehicle have been studied in Ref. 4.

The study of the minimum-time maneuvering problem in the horizontal plan is done in three steps:

1) The minimum principle and the associated two-point boundary-value problem (TPBVP) are formulated and numerically solved by a multiple shooting algorithm.

2) The Jacobi test is carried out by a technique based on singular-value decomposition.

3) An approximation scheme is considered, in which we assume constant flight speed along the trajectories.

In both, the exact and the approximate formulation the altitude is assumed to be kept constant by the longitudinal control loops. The vehicle is of a bank-to-turn type, and therefore, the bank angle is the natural controller for this problem.

Problem Statement

The equations of motion for a point-mass model of the vehicle are

$$\begin{aligned} \dot{x} &= V\cos\Psi \\ \dot{y} &= V\sin\Psi \\ \dot{e} &= (V/W)(Th - D) \\ \dot{\Psi} &= (g/V)\tan\Phi \end{aligned} \tag{1}$$

In this formulation, we assume constant mass, zero skid angle, thrust directed along the flight path, and constant altitude. The bank angle Φ is taken to be the control variable. The velocity V is related to the specific energy by

$$e = h + V^2/2g \tag{2}$$

We further assume a drag polar of the form

$$D = D0 + Di\,n^2 \tag{3}$$

where

$$n = 1/\cos\Phi \tag{4}$$

$$D0 = qSCd0, \qquad Di = KW/qS \tag{5}$$

The propulsive force is of the form

$$Th = k\delta(A1\beta^2 + A2\beta + A3), \qquad A1 > 0 \tag{6}$$

where k, $A1$, $A2$, and $A3$ are empirical constants, and where

$$\begin{aligned} \delta &= Pt/P0 \\ \beta &= (T0/Tt)^2 \end{aligned} \tag{7}$$

The models for the aerodynamics and for the propulsive forces have been confirmed by ground tests (wind-tunnel and altitude chamber tests) and by flight tests. The control variable Φ is bounded by

$$\Phi_{min} \le \Phi \le \Phi_{max} \tag{8}$$

Presented as Paper 92-4344 at the AIAA Flight Mechanics Conference, Hilton Head, SC, Aug. 10–12, 1992; received Oct. 3, 1993; revision received July 4, 1994; accepted for publication July 5, 1994.

*Head of Control Department, Advanced Systems Division, P.O. Box 1044-77. Member AIAA.

Table 1 System parameters

	Propulsion				Aerodynamics			Control	
W, lb	k	$A1$	$A2$	$A3$	$Cd0$	K	S	Φ_{min}	Φ_{max}
400	0.96 lb	281.8	−94.1	−56.9	0.065	0.16	3.47 ft^2	−0.8726, −50 deg	0.8726, 50 deg

We shall employ standard atmospheric properties to model the ambient temperature, the air density and the atmospheric pressure.

The optimal control problem is to determine the control variable which, subject to the constraint (8), will drive the system (1) from a given initial condition to a predetermined terminal position and azimuth. The terminal energy (i.e., velocity) is free, and the cost is the transition time

$$J = Tf \tag{9}$$

Problem Analysis

First-Order Conditions

We define the Hamiltonian

$$H \equiv 1 + \lambda_x \dot{x} + \lambda_y \dot{y} + \lambda_e \dot{e} + \lambda_\Psi \dot{\Psi} \tag{10}$$

First-order necessary conditions (including transversality conditions) are of the form[5]

$$\dot{\lambda}_i = -\frac{\partial H}{\partial x_i} \tag{11}$$

$$\begin{aligned} H(Tf) &= 0 \\ \lambda_e(Tf) &= 0 \end{aligned} \tag{12}$$

By the minimum principle the Hamiltonian has to be minimized by the control, thus

$$\frac{\partial H}{\partial \Phi} = 0 \tag{13}$$

hence

$$\tan \Phi = (gW/2DiV^2)(\lambda_\Psi/\lambda_e) \tag{14}$$

If, however, Eq. (8) is violated, the specified limit should be taken.

Second-Order Condition

A second-order necessary condition, the Jacobi condition, is considered next. We employ the approach of Kelley and Moyer[6,7] of evaluating the rank of the transition matrix $G(t)$ defined by

$$\delta \bar{x}(t) = G(t)\delta \bar{\lambda}(0) \tag{15}$$

where $\delta\bar{\lambda}(0)$ is a perturbation in the initial value of the costate vector, and $\delta\bar{x}$ is the resulting perturbation in the state vector, thus

$$G(t) \equiv \begin{bmatrix} \frac{\partial x(t)}{\partial \lambda_x(0)} & \frac{\partial x(t)}{\partial \lambda_y(0)} & \frac{\partial x(t)}{\partial \lambda_e(0)} & \frac{\partial x(t)}{\partial \lambda_\Psi(0)} \\ \frac{\partial y(t)}{\partial \lambda_x(0)} & \frac{\partial y(t)}{\partial \lambda_y(0)} & \frac{\partial y(t)}{\partial \lambda_e(0)} & \frac{\partial y(t)}{\partial \lambda_\Psi(0)} \\ \frac{\partial e(t)}{\partial \lambda_x(0)} & \frac{\partial e(t)}{\partial \lambda_y(0)} & \frac{\partial e(t)}{\partial \lambda_e(0)} & \frac{\partial e(t)}{\partial \lambda_\Psi(0)} \\ \frac{\partial \Psi(t)}{\partial \lambda_x(0)} & \frac{\partial \Psi(t)}{\partial \lambda_y(0)} & \frac{\partial \Psi(t)}{\partial \lambda_e(0)} & \frac{\partial \Psi(t)}{\partial \lambda_\Psi(0)} \end{bmatrix} \tag{16}$$

Table 2 Boundary conditions

$x(0)$	$x(Tf)$	$y(0)$	$y(Tf)$	$\Psi(0)$	$\Psi(Tf)$
		Case a, ft			
0	50,000	0	200	0	0
		Case b, ft			
0	50,000	0	2,000	0	0
		Case c, ft			
0	50,000	0	20,000	0	0

Due to the fact that $\delta\bar{x}$ is normal to the costate vector $\bar{\lambda}$,[6,7] the rank of this matrix is less than four, when evaluated around an extremal [i.e., a solution to Eqs. (11–14)]. A drop in the rank from three to two (or less) indicates a conjugate point, and a nonoptimal extremal. In order to carry out this test one has to accomplish two tasks: 1) constructing the matrix $G(t)$ and 2) evaluating the rank of $G(t)$.

A simple way to accomplish the first task is by direct numerical differentiation,[6,7] which requires n additional integrations of the system equations. On each integration, we change one of the costates at the initial time by a small amount. The "smallness" of this perturbation should be verified by checking the linearity of the solution. As in the previous work,[4] we use a singular-value decomposition (SVD)[8] for the second task. This is numerically preferable[9] over computing the determinants of the minors of $G(t)$ as originally suggested in Ref. 6. In this approach we evaluate and plot the singular values of $G(t)$ as a function of time. One singular value should vanish, but the other three should be different than zero, thus indicating one-dimensional null space. It should be noted that the numerical value of the "zero" singular value is a measure of the "smallness" of the perturbation taken to construct $G(t)$. Having an extremal that satisfies the minimum principle and the Jacobi condition on $0 < t \leq Tf$, one may claim that sufficient conditions for local optimality have been obtained.[5]

Numerical Examples

Numerical values for the DELILAH system are given in Table 1. Three numerical examples have been studied employing offset maneuvers. The initial conditions and the target points are listed in Table 2. The altitude has been fixed to 10,000 ft, and the initial specific energy to 20,000 ft. Extremals for the associated TPBVP have been obtained by a multiple-shooting algorithm, where initial costate vectors of smaller offset maneuvers were used as guesses for the larger maneuvers. The optimal control time histories for all three cases are shown (in normalized time) in Fig. 1. The optimal costs (transition times) are 65.8, 65.9, and 72.9 s for case a, case b, and case c, respectively. In all cases the solution seems to possess two boundary layers, one near the beginning and one near the end, where bank-to-turn maneuvers are taking place. In the intermediate phase the bank angle is relatively small and the flight is almost straight and level. The initial turn is always gradual whereas the final turn is very fast. The reason for that is the importance of maintaining speed during early stages of the flight. Tight turns should therefore be avoided. This is no longer valid at the final boundary layer where tight turns are desirable. Notice that in case a, the least demanding case in terms of the cross-track offset, the control does not reach its limits in any of the boundary layers; in the more demanding

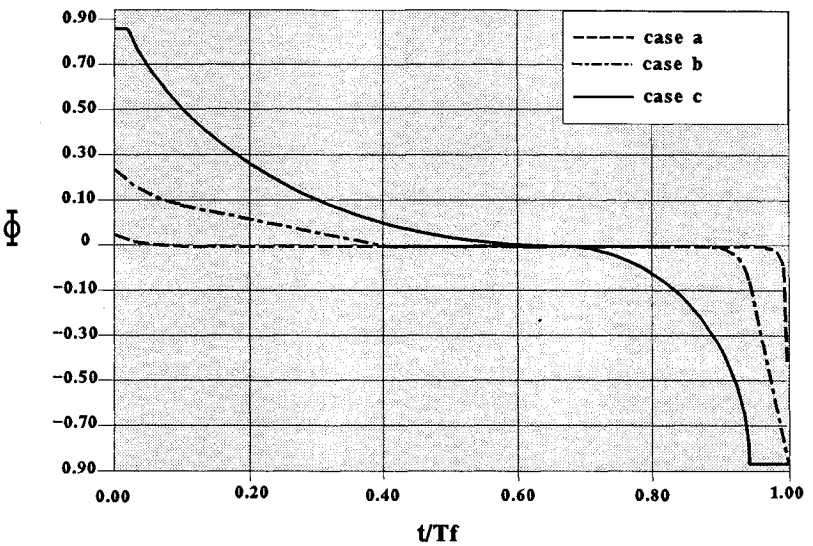

Fig. 1 Optimal control time histories.

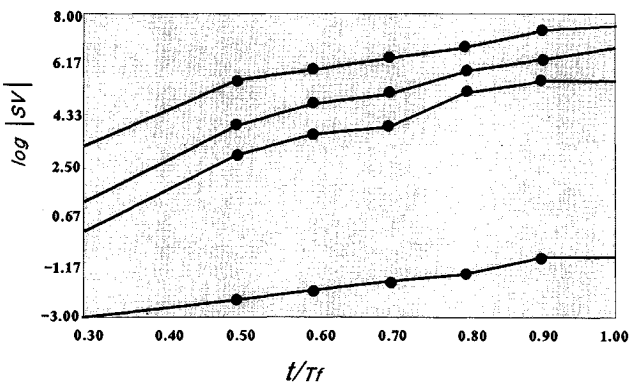

Fig. 2 Singular values.

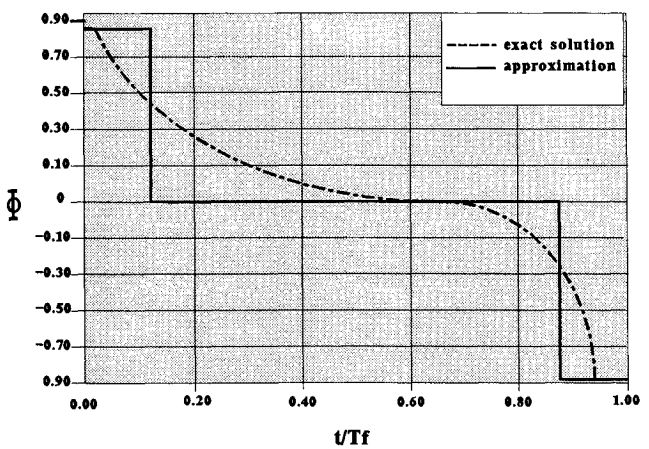

Fig. 3 Approximate vs exact solutions.

case, case b, it reaches its bound in the terminal boundary layer; whereas in the most demanding case, case c, the maximal values have been applied both at the beginning and at the end of the trajectory.

In order to test for conjugate points, we have perturbed the trajectories, as explained above, by varying the initial value of the costate vector. The linearity of each perturbed trajectory has been checked numerically. The singular values of the matrix $G(t)$ for case c are shown in Fig. 2 on a logarithmic scale. For presentation purposes the singular values are shown for $t \geq 0.3Tf$. They increase monotonically on the interval $0 \leq t \leq 0.3Tf$.) As expected, there is a numerical "zero" singular value, whereas the remaining singular values are all within several orders of magnitude higher. In general, the nonzero singular values seem to blow up as time unfolds. A similar result has been observed in Ref. 4.

Approximation Scheme

The computational burden of solving two-point boundary value problems, such as the minimum-time intercept with the point-mass model, may be very significant when one begins with no previous knowledge about the adjoints. This is especially true for onboard implementations of the optimization algorithms. This unfortunate fact provides the motivation for the approximation method that will be considered next. Assuming constant speed, the state-space is reduced to three:

$$\begin{aligned} \dot{x} &= V\cos\Psi \\ \dot{y} &= V\sin\Psi \\ \dot{\Psi} &= (g/V)\tan\Phi \end{aligned} \tag{17}$$

The optimal control should satisfy

$$\Phi = \begin{cases} \Phi_{\max} & \lambda_\Psi < 0 \\ 0 & \lambda_\Psi = 0 \\ \Phi_{\min} & \lambda_\Psi > 0 \end{cases} \tag{18}$$

The singular control is obtained from the requirements $d\lambda_\Psi/dt = 0$, $d^2\lambda_\Psi/t^2 = 0$.

For our numerical example the constant speed was fixed to 750 fps, which is the cruise speed at this altitude. The optimal controls have been all of the bang-singular-bang type (this is the common situation, but not the only one possible[2]), which is in qualitative agreement with the exact solutions. The optimal costs are 66.70, 66.72, and 72.26 s for cases a, b, and c, respectively. A comparison of an approximate control function (case c), with the exact solution is shown in Fig. 3. The results are in reasonably good agreement. The computational effort in solving the exact problem is significantly higher than the approximate one; in fact the latter is simple enough to be considered for onboard implementations.[2]

Conclusions

Pontryagin minimum principle has been applied to a minimum-time point-to-point maneuvering problem of a bank-to-turn UAV. The Jacobi test has been performed, by a reliable SVD technique, to check for the optimality of the solutions. Numerical studies revealed a typical pattern of

minimum-time trajectories with three time-zones of azimuth changing. A mild turn at the beginning, an almost level flight, and a final tight turn. An approximation to the problem, with a constant-speed assumption, has been shown to be in good agreement with the exact solution.

References

[1]Kelley, H. J., "Aircraft Maneuver Optimization by Reduced-Order Approximations," *Control and Dynamics Systems*, Vol. X, edited by C. T. Leondes, Academic, New York, 1973.

[2]Erzberger, H., and Lee, H. Q., "Optimum Horizontal Guidance Technique for Aircraft," *Journal of Aircraft*, Vol. 8, No. 2, 1971, pp. 95–101.

[3]Guelman, M., and Shinar, J., "Optimal Guidance Law in the Plane," *Journal of Guidance, Control, and Dynamics*, Vol. 7, No. 4, 1984, pp. 471–476.

[4]Ben-Asher, J. Z., "Optimal Trajectories for an Unmanned Air-Vehicle," *Proceedings of the 31st Israel Conference on Aviation and Astronautics*, 1990, pp. 132–139.

[5]Bryson, A. E., and Ho, Y.-C., *Applied Optimal Control*, Hemisphere, Washington, DC, 1975.

[6]Kelley, H. J., and Moyer, H. G., "Computational Jacobi Test Procedure," JURFMA Workshop on Current Trend in Control, Dubrovnik, Yugoslavia, June 1984.

[7]Moyer, H. G., "Optimal Control Problems that Test for Envelope Contacts," *Journal of Optimization Theory and Applications*, Vol. 6, No. 4, 1976, pp. 287–298.

[8]Ben-Asher, J. Z., and Cliff, E. M., "The Jacobi Test and Its Numerical Implementations," Virginia Tech, ICAM Rept.

[9]Lawson, C. L., and Hanson, R. J., *Solving Least-Square Problems*, Prentice–Hall, Englewood Cliffs, NJ, 1974.

Effect of Leading-Edge Extension Fences on the Vortex Wake of an F/A-18 Model

Sheshagiri K. Hebbar* and Max F. Platzer†
Naval Postgraduate School, Monterey, California 93943
and
William D. Frink Jr.‡
CAS Inc., Huntsville, Alabama 35814

Introduction

ONE of the topics of current interest in high angle-of-attack (AOA) aerodynamic research is the interaction between the F/A-18's leading-edge extension (LEX) vortex and the vertical tail surfaces. The resulting buffeting of the vertical tails has led to the development and implementation of a LEX fence for the F/A-18. Recent investigations of vertical tail buffet of the F/A-18 aircraft, both in wind-tunnel tests[1–3] and flight tests,[4] have shown that the LEX fence has little effect on the position of vortex burst, but causes formation of a second vortex near the fence and reduces the dynamic loading on the vertical tail. Brief reviews of the previous studies related to tail buffeting phenomena on twin-tailed aircraft at high AOA appear in Refs. 5 and 6. Data on spectral energy content of the vortex, both with and without LEX fences, will significantly add to the understanding of vortex/tail surface interaction. To this end, an investigation was conducted in the Naval Postgraduate School (NPS) 32- by 45-in. low-speed wind tunnel, using a 3% scale model of the Northrop YF-17, the lightweight prototype from which the F/A-18 was evolved.[7] The results of the hot-wire surveys of the downstream wake with and without LEX fences are discussed, with particular emphasis on power spectral data. Additional details of the investigation appear in Refs. 7 and 8.

Experimental Program

The NPS tunnel is a closed-circuit, single-return, horizontal-flow wind tunnel with a contraction ratio of 10:1, a test section 1.143 m wide by 0.813 m high by 1.219 m long, a maximum test section velocity of 80 m/s, and a nominal free-stream turbulence level of 0.2%. A yoke assembly attached to a horizontal turntable located in the center of the test section floor permits sting-mounting of the model and variable pitch angles (Fig. 1). The diameters of the sting and the vertical strut were 15.9 and 25.4 mm, respectively, and the distance of the vertical strut to rear of the model was 0.133 m. The 3% YF-17 model having a length of 0.486 m, a wingspan of 0.32 m and a mean aerodynamic chord (MAC) of 0.098 m was chosen due to its close similarity to the F/A-18 and its availability. Dissimilarities between the YF-17 and the F/A-18 were considered minor enough in the investigation of the effects of the LEX fence.[7–9] The model was configured with neutral flap settings and wingtip missiles. Note that the same model was tested in Ref. 5, but without wingtip missiles. The 3% scaled version of the NASA Ames LEX fences was constructed from 0.8-mm-thick balsa wood and installed one on each side of the model near the junction of the LEX and the wing.[8]

Flow visualization by injection of smoke into the test section at low tunnel velocities (5–10 m/s) helped determine the approximate location of vortices downstream of the model. This information was subsequently used to determine locations for hot-wire surveys. The crossprobe was mounted on a traversing mechanism (Fig. 1) that allowed surveying laterally by turning the traversing crank. A spectrum analyzer provided spectrum

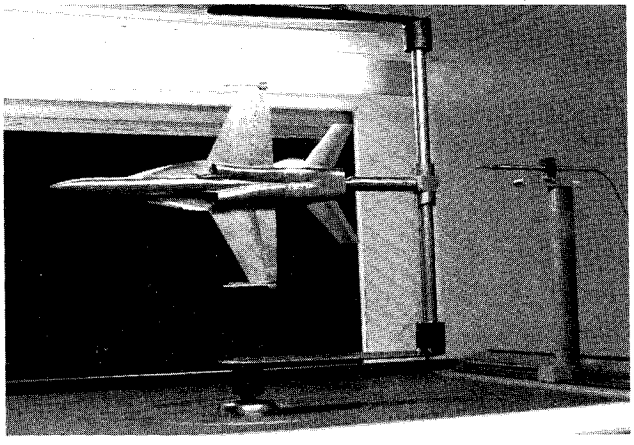

Fig. 1 Model in the NPS wind tunnel with hot-wire probe at station B.

Presented as Paper 93-0868 at the AIAA 31st Aerospace Sciences Meeting and Exhibit, Reno, NV, Jan. 11–14, 1993; received Feb. 23, 1994; revision received Sept. 28, 1994; accepted for publication Sept. 28, 1994.

*Adjunct Professor, Department of Aeronautics and Astronautics. Associate Fellow AIAA.

†Professor, Department of Aeronautics and Astronautics. Associate Fellow AIAA.

‡Senior Systems Engineer, Systems Engineering Department.